J. Fluid Mech. (1989), *vol.* 205, *pp.* 163–170
Printed in Great Britain

A note on long waves induced by short-wave groups over a shelf

By PHILIP L.-F. LIU

Joseph H. DeFrees Hydraulic Laboratory, School of Civil and Environmental Engineering, Cornell University, Ithaca, NY 14853, USA

(Received 3 May 1988 and in revised form 27 September 1988)

The generation of long waves due to the refraction of wave groups over a shelf is re-examined. The appropriate boundary conditions for calculating the second-order mean free-surface displacement are discussed. Numerical results for a plane shelf are presented, which are different from those given by Mei & Benmoussa (1984).

1. Introduction

Mei & Benmoussa (1984, hereafter referred to as M & B) studied the long waves induced by short-wave groups over an uneven bottom. They showed that as the wave groups are refracted over a slowly varying depth region, two types of long waves, locked long waves and free long waves, are generated. While the locked long waves propagate together with the envelope of the short waves at their group velocity, the free long waves are radiated away from the varying-depth region at the shallow water speed, $(gh)^{\frac{1}{2}}$. M & B gave numerical results for several different one-dimensional topographies, including a linear shelf connecting two water depths. The depth slope is discontinuous at the edges of the shelf.

In M & B's analysis only part of the second-order mean free-surface displacements and the normal flux are required to be continuous at the edges of the shelf. Because of the discontinuities in depth slope, the forcing terms (momentum fluxes) for the second-order free-surface displacements are also discontinuous along the edges of the linear shelf. In this note, we re-examine the problem and derive proper matching conditions along the edges of the shelf. It is shown numerically that the depth discontinuity is also a source of generating long waves.

In the following section we first summarize M & B's theory and give the corrections to some of the typographical errors which appeared in M & B. An alternative solution method for the long waves is given in §3. Numerical results are shown in §4.

2. Summary of M & B's theory

In this section we summarize the theory and key equations presented in M & B. In the original paper, some of these equations contain typographical errors, which are corrected here. M & B's original equation number is co-listed, when corrections have been made.

Denoting ζ as the first-order free-surface displacement,

$$\zeta = \tfrac{1}{2}A \exp\left[\mathrm{i}\left(\int^{x} \boldsymbol{k}(\boldsymbol{x})\cdot \mathrm{d}\boldsymbol{x} - \omega t\right)\right] + *, \tag{2.1}$$

in which * denotes the complex conjugate of the preceding term, $A(X, T)$ is the amplitude, ω is the wave frequency, $\boldsymbol{k}$ is the wavenumber vector, and ξ is the second-order mean free-surface displacement, the governing equations for A and ξ are given as

$$\frac{\partial A^2}{\partial T}+\nabla\cdot(C_g A^2)=0, \quad \nabla=\left(\frac{\partial}{\partial X},\frac{\partial}{\partial Y}\right), \tag{2.2}$$

(M & B 2.6)

$$\nabla\cdot(h\nabla\xi)-\frac{\partial^2\xi}{\partial T^2}=\frac{\partial}{\partial T}\nabla\cdot\left(\frac{\boldsymbol{k}|A|^2}{2}\right)-\nabla\cdot\left[h\nabla\left(\frac{|A|^2}{4\sinh^2 kh}\right)\right]. \tag{2.3}$$

Note that $(X, Y, T)=\epsilon(x, y, t)$, where $\epsilon \ll 1$, are the slow variables and equations (2.1)–(2.3) are dimensionless. The non-dimensional variables are defined in (2.12) of M & B. To be consistent with the equations used in M & B and this note, the second-order mean free-surface displacement should be, however, normalized by the characteristic wave height (twice the wave amplitude a_0), $2a_0$, i.e.

$$\xi\to k_\infty(2a_0)^2\xi. \tag{2.4}$$

(M & B 2.12)

M & B assumed that the incident wave groups are the superposition of two colinear sinusoidal wave trains of slightly different wavenumbers, $\boldsymbol{k}\pm\epsilon\boldsymbol{k}_0$, with normalized amplitudes 1 and b, respectively. The wave amplitude over the region of variable depth, $h(X)$, can be written as

$$A(X,Y,T)=\tilde{A}(X)\left\{\exp\left[\mathrm{i}\left(\int_{X_0}^{X}K_x\,\mathrm{d}X+k_y Y-\Omega T\right)\right]+b\exp\left[-\mathrm{i}\left(\int_{X_0}^{X}K_x\,\mathrm{d}X+k_y Y-\Omega T\right)\right]\right\}, \tag{2.5}$$

(M & B 3.5)

where the amplitude $\tilde{A}(X)$ and the x-component of the wavenumber for the wave envelope, K_x, can be expressed as

$$\tilde{A}(X)=\left[\frac{C_{gx0}}{C_{gx}}\right]^{\frac{1}{2}}, \tag{2.6}$$

$$K_x=k_x+\frac{k^2}{k_x}\left(\frac{CC_{g0}}{C_0C_g}-1\right). \tag{2.7}$$

(M & B 3.9)

We remark here that a factor of $\frac{1}{2}$ was included in M & B's (3.5) for the expression of the wave amplitude, A. As a result their equation represented the superposition of two sinusoidal wave trains with normalized amplitude $\frac{1}{2}$ and $\frac{1}{2}b$, respectively. The second-order free-surface displacement, corresponding to (2.5)–(2.7), can be written as:

$$\xi=\xi_0(X)+\tfrac{1}{2}\{\tilde{\xi}(X)\exp[2\mathrm{i}(k_y Y-\Omega T)]+*\}. \tag{2.8}$$

In (2.8) $\xi_0(X)$ represents the steady-state component of the second-order free-surface displacement, i.e.

$$\xi_0(X)=-\frac{(1+b^2)|\tilde{A}|^2}{16\sinh^2 kh}. \tag{2.9}$$

The dynamic component $\tilde{\xi}$ is governed by

$$\frac{\mathrm{d}}{\mathrm{d}X}\left(h\frac{\mathrm{d}\tilde{\xi}}{\mathrm{d}X}\right)+4(\Omega^2-k_y^2h)\,\tilde{\xi}=\left\{\left[\frac{h(K_x^2+k_y^2)}{2\,\mathrm{sh}^2kh}+\frac{\Omega^2k}{C_g}\right]\frac{bC_{gx0}}{C_{gx}}\right.$$
$$+\frac{2b}{1+b^2}\left[\frac{\mathrm{d}}{\mathrm{d}X}\left(h\frac{\mathrm{d}\xi_0}{\mathrm{d}X}\right)+\mathrm{i}\left(4K_xh\frac{\mathrm{d}\xi_0}{\mathrm{d}X}+2\xi_0\frac{\mathrm{d}}{\mathrm{d}X}(K_xh)\right)\right]$$
$$\left.-\tfrac{1}{2}\mathrm{i}b\,\Omega C_{gx0}\frac{\mathrm{d}}{\mathrm{d}X}\left(\frac{k}{C_g}\right)\right\}\exp\left(2\mathrm{i}\int_{X_0}^{X}K_x\,\mathrm{d}X\right). \tag{2.10}$$

(M & B 3.15)

For constant depth the above equation can be integrated to give the locked long waves

$$\tilde{\xi}=\xi_L\exp\left(2\mathrm{i}\int_{X_0}^{X}K_x\,\mathrm{d}X\right), \tag{2.11}$$

with

$$\xi_L=-\frac{bC_{gx0}}{4C_{gx}}\left[\frac{h(K_x^2+k_y^2)}{2\,\mathrm{sh}^2kh}+\frac{\Omega^2k}{C_g}\right][h(K_x^2+k_y^2)-\Omega^2]^{-1}. \tag{2.12}$$

(M & B 4.2)

For $b=1$ and normal incidence, ξ_L reduces to

$$\xi_L=-\frac{4k_0C_{g0}-1}{8(h_0-C_{g0}^2)}. \tag{2.13}$$

(M & B 4.3)

In the constant-depth regions, $X_1<X$ or $X<X_0$, the complete solutions for $\tilde{\xi}$ are of the form

$$\tilde{\xi}=(\xi_L)_j\exp\left(2\mathrm{i}\int_{X_0}^{X}K_x\,\mathrm{d}X\right)+(\xi_F)_j, \tag{2.14}$$

where $j=0$ corresponds to $X<X_0$ and $j=1$ to $X>X_1$. In (2.14) $(\xi_L)_j$ ($j=0$ and 1) are given in (2.12), while $(\xi_F)_j$ are the free long waves which are the homogeneous solutions of (2.10) over the constant depth h_0 and h_1. Because the free long waves must be either outgoing waves propagating away or decaying exponentially from the region of variable depth, the general expression for ξ_F may be written as

$$(\xi_F)_j=B_j\exp\left[2\mathrm{i}(-1)^{j+1}\lambda_j(X-X_j)\right]. \tag{2.15}$$

where

$$\lambda_j^2=\frac{1}{h_j}(\Omega^2-k_y^2h_j)=k_0^2\left(\frac{C_{g0}^2}{h_j}-\sin^2\alpha_0\right). \tag{2.16}$$

(M & B 4.5)

Note that λ_j could be real or imaginary.

Over the region of variable depth, $X_0<X<X_1$, M & B suggested that the dynamic mean free-surface displacement could be expressed as

$$\tilde{\xi}=\xi_L\exp\left(2\mathrm{i}\int_{X_0}^{X}K_x\,\mathrm{d}X\right)+\xi_F. \tag{2.17}$$

The governing equation for ξ_F is

$$\frac{\mathrm{d}}{\mathrm{d}X}\left(h\frac{\mathrm{d}\xi_F}{\mathrm{d}X}\right)+4(\Omega^2-k_y^2h)\,\xi_F=G(X), \tag{2.18}$$

where

$$G(X) = \left\{\frac{2b^2}{1+b^2}\left[h\frac{\mathrm{d}^2 Z}{\mathrm{d}X^2}+\frac{\mathrm{d}h}{\mathrm{d}X}\frac{\mathrm{d}Z}{\mathrm{d}X}+\mathrm{i}\left(4hK_x\frac{\mathrm{d}Z}{\mathrm{d}X}+2Z\frac{\mathrm{d}}{\mathrm{d}X}(K_x h)\right)\right]\right.$$
$$\left.-\tfrac{1}{2}\mathrm{i}b\,C_{g0}^2 k_0\cos\alpha_0\frac{\mathrm{d}}{\mathrm{d}X}\left(\frac{k}{C_g}\right)\right\}\exp\left(2\mathrm{i}\int_{X_0}^{X}K_x\,\mathrm{d}X\right), \qquad (2.19)$$

(M & B 5.2)

and $Z = \xi_0 - \xi_L$. M & B solved (2.18) numerically with the following boundary conditions:

$$\xi_F = (\xi_F)_j, \quad \frac{\mathrm{d}\xi_F}{\mathrm{d}X} = \frac{\mathrm{d}(\xi_F)_j}{\mathrm{d}X}, \quad \text{at } X = X_j, \qquad (2.20)$$

where $(\xi_F)_j$ is given in (2.15). The first boundary condition ensures the continuity of the total second-order free-surface displacement. The second matching condition in (2.20) is, however, somewhat arbitrary for the cases with discontinuities in depth slopes.

For cases where the bottom slope is discontinuous at X_0 and/or X_1, the first derivative of ξ_0, ξ_L as well as the forcing terms of the second-order free-surface displacement (the right-hand side of (2.10)) are also discontinuous. The matching conditions given in (2.20) are inconsistent with the governing equation for $\tilde{\xi}$, (2.10), along the edges of the shelf. The appropriate matching (jump) condition for $\mathrm{d}\tilde{\xi}/\mathrm{d}x$ at $X = X_0$ can be obtained by integrating (2.10) from $X = X_0 - \delta$ to $X_0 + \delta$ and taking the limit as $\delta \to 0$. Hence,

$$\left[\frac{\mathrm{d}\tilde{\xi}}{\mathrm{d}X}\right]_{X_0} = \left.\frac{\mathrm{d}\tilde{\xi}}{\mathrm{d}X}\right|_{X_0+} - \left.\frac{\mathrm{d}\tilde{\xi}}{\mathrm{d}X}\right|_{X_0-}$$
$$= \frac{2b}{1+b^2}\left[\frac{\mathrm{d}\xi_0}{\mathrm{d}X}\right]_{X_0} = \frac{2b}{1+b^2}\left[\left.\frac{\mathrm{d}\xi_0}{\mathrm{d}X}\right|_{X_0+} - \left.\frac{\mathrm{d}\xi_0}{\mathrm{d}X}\right|_{X_0-}\right], \qquad (2.21)$$

in which $X_0 \pm = \lim(X_0 \pm \delta)$, as $\delta \to 0$. Similarly, the jump condition for $\mathrm{d}\tilde{\xi}/\mathrm{d}x$ at $X = X_1$ can be found as

$$\left[\frac{\mathrm{d}\tilde{\xi}}{\mathrm{d}X}\right]_{X_1} = \left.\frac{\mathrm{d}\tilde{\xi}}{\mathrm{d}X}\right|_{X_1+} - \left.\frac{\mathrm{d}\tilde{\xi}}{\mathrm{d}X}\right|_{X_1-}$$
$$= \frac{2b}{1+b^2}\left[\frac{\mathrm{d}\xi_0}{\mathrm{d}X}\right]_{X_1}\exp\left(2\mathrm{i}\int_{X_0}^{X_1}K_x\,\mathrm{d}X\right)$$
$$= \frac{2b}{1+b^2}\left[\left.\frac{\mathrm{d}\xi_0}{\mathrm{d}X}\right|_{X_1+} - \left.\frac{\mathrm{d}\xi_0}{\mathrm{d}X}\right|_{X_1-}\right]\exp\left(2\mathrm{i}\int_{X_0}^{X_1}K_x\,\mathrm{d}X\right), \qquad (2.22)$$

in which $X_1 \pm = \lim(X_1 \pm \delta)$, as $\delta \to 0$.

3. An alternative solution method

As pointed out by M & B, because of the appearance of the first- and second-derivatives of ξ_0 and ξ_L on the right-hand side of (2.18), double precision is necessary in their numerical scheme. We remark that the slope of ξ_L at $h = 0.5$ is very steep, nearly vertical. To avoid this numerical accuracy problem, we solve (2.18) after a simple transformation. Introducing the transformation

$$F(X) = \tilde{\xi} - \frac{2b}{1+b^2}\xi_0\exp\left(2\mathrm{i}\int_{X_0}^{X}K_x\,\mathrm{d}X\right) \qquad (3.1)$$

into (2.10), we obtain

$$\frac{\mathrm{d}}{\mathrm{d}X}\left(h\frac{\mathrm{d}F}{\mathrm{d}X}\right)+4(\Omega^2-k_y^2h)F=\mathbb{D}(X), \tag{3.2}$$

in which

$$\mathbb{D}(X)=\left\{\Omega^2\left[\frac{1}{2\sinh^2 kh}+\frac{k}{C_g}\right]\frac{bC_{gx0}}{C_{gx}}-\tfrac{1}{2}\mathrm{i}b\,\Omega C_{gx0}\frac{\mathrm{d}}{\mathrm{d}X}\left(\frac{k}{C_g}\right)\right\}\exp\left(2\mathrm{i}\int_{X_0}^{X}K_x\,\mathrm{d}X\right), \tag{3.3a}$$

$$\frac{\mathrm{d}}{\mathrm{d}X}\left(\frac{k}{C_g}\right)=\frac{k}{hC_g}\frac{\mathrm{d}h}{\mathrm{d}X}\left(\frac{1}{2}\frac{C}{C_g}-1\right)\left[1+\frac{C}{C_g}(1-h)\right]. \tag{3.3b}$$

Therefore, the right-hand side of (3.2) does not involve the derivatives of ξ_0 and ξ_L. The boundary conditions used to solve (3.2) are the continuity of the total $\tilde{\xi}$ defined in (2.17) and the jump conditions for $\mathrm{d}\tilde{\xi}/\mathrm{d}x$ at $X=X_0$ and X_1 as given in (2.21) and (2.22). Thus

$$F(X_0)+\frac{2b}{1+b^2}\xi_0=\xi_L+B_0, \tag{3.4}$$

$$\frac{\mathrm{d}F}{\mathrm{d}X}+\left(\frac{2b}{1+b^2}\right)2\mathrm{i}K_x\xi_0=2\mathrm{i}K_x\xi_L-2\mathrm{i}\lambda_0B_0-\left(\frac{2b}{1+b^2}\right)\frac{\mathrm{d}\xi_0}{\mathrm{d}X}\bigg|_{X_0-}, \tag{3.5}$$

at $X=X_0$, and

$$F(X_1)+\frac{2b}{1+b^2}\xi_0\exp\left(2\mathrm{i}\int_{X_0}^{X_1}K_x\,\mathrm{d}X\right)=\xi_L\exp\left(2\mathrm{i}\int_{X_0}^{X_1}K_x\,\mathrm{d}X\right)+B_1, \tag{3.6}$$

$$\frac{\mathrm{d}F}{\mathrm{d}X}+\left(\frac{2b}{1+b^2}\right)2\mathrm{i}K_x\xi_0\exp\left(2\mathrm{i}\int_{X_0}^{X_1}K_x\,\mathrm{d}X\right)$$
$$=\left[2\mathrm{i}K_x\xi_L-\left(\frac{2b}{1+b^2}\right)\frac{\mathrm{d}\xi_0}{\mathrm{d}X}\bigg|_{X_1+}\right]\exp\left(2\mathrm{i}\int_{X_0}^{X_1}K_x\,\mathrm{d}X\right)+2\mathrm{i}\lambda_1B_1, \tag{3.7}$$

at $X=X_1$. Eliminating B_0 from (3.4) and (3.5), we obtain

$$\frac{\mathrm{d}F}{\mathrm{d}X}+2\mathrm{i}\lambda_0F=2\mathrm{i}\,(K_x+\lambda_0)\left[\xi_L-\left(\frac{2b}{1+b^2}\right)\xi_0\right]-\left(\frac{2b}{1+b^2}\right)\frac{\mathrm{d}\xi_0}{\mathrm{d}X}\bigg|_{X_0-}, \tag{3.8}$$

at $X=X_0$. From (3.6) and (3.7), we can eliminate B_1 to get

$$\frac{\mathrm{d}F}{\mathrm{d}X}-2\mathrm{i}\lambda_1F=\left\{2\mathrm{i}\,(K_x-\lambda_1)\left[\xi_L-\left(\frac{2b}{1+b^2}\right)\xi_0\right]-\left(\frac{2b}{1+b^2}\right)\frac{\mathrm{d}\xi_0}{\mathrm{d}X}\bigg|_{X_1+}\right\}\exp\left(2\mathrm{i}\int_{X_0}^{X_1}K_x\,\mathrm{d}X\right), \tag{3.9}$$

at $X=X_1$. Equation (3.2) with the boundary conditions (3.8) and (3.9) can be readily solved by a finite-difference method. Once F is found, B_0 and B_1 can be calculated from (3.4) and (3.6).

4. Numerical examples

In this section numerical results are presented for the case of a linear shelf in which a plane slope connects two constant depths. Mathematically, these shelves can be expressed as

$$h(X)=h_0+(X-X_0)\,(h_1-h_0)/(X_1-X_0), \tag{4.1}$$

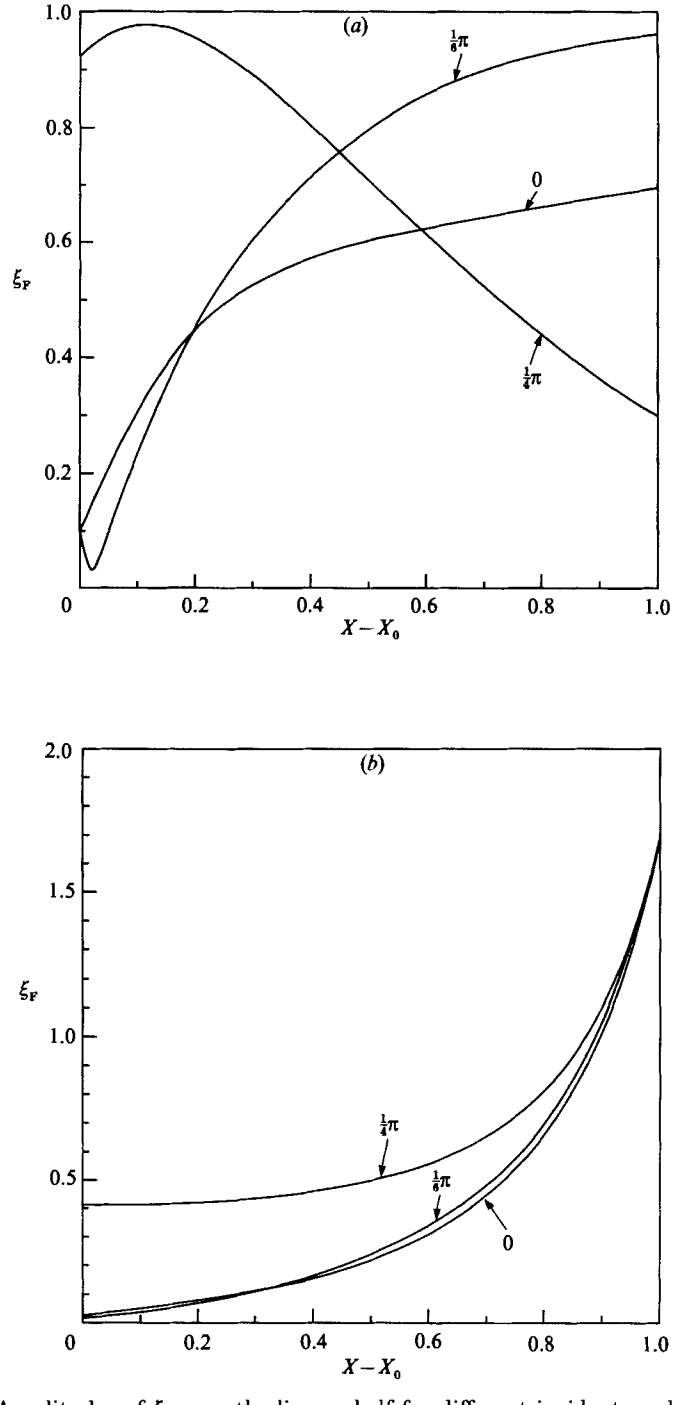

FIGURE 1. Amplitudes of ξ_F over the linear shelf for different incident angles with $|h_1-h_0| = 0.5$: (*a*) $h_0 = 0.5$ and $h_1 = 1.0$; (*b*) $h_0 = 1.0$ and $h_1 = 0.5$.

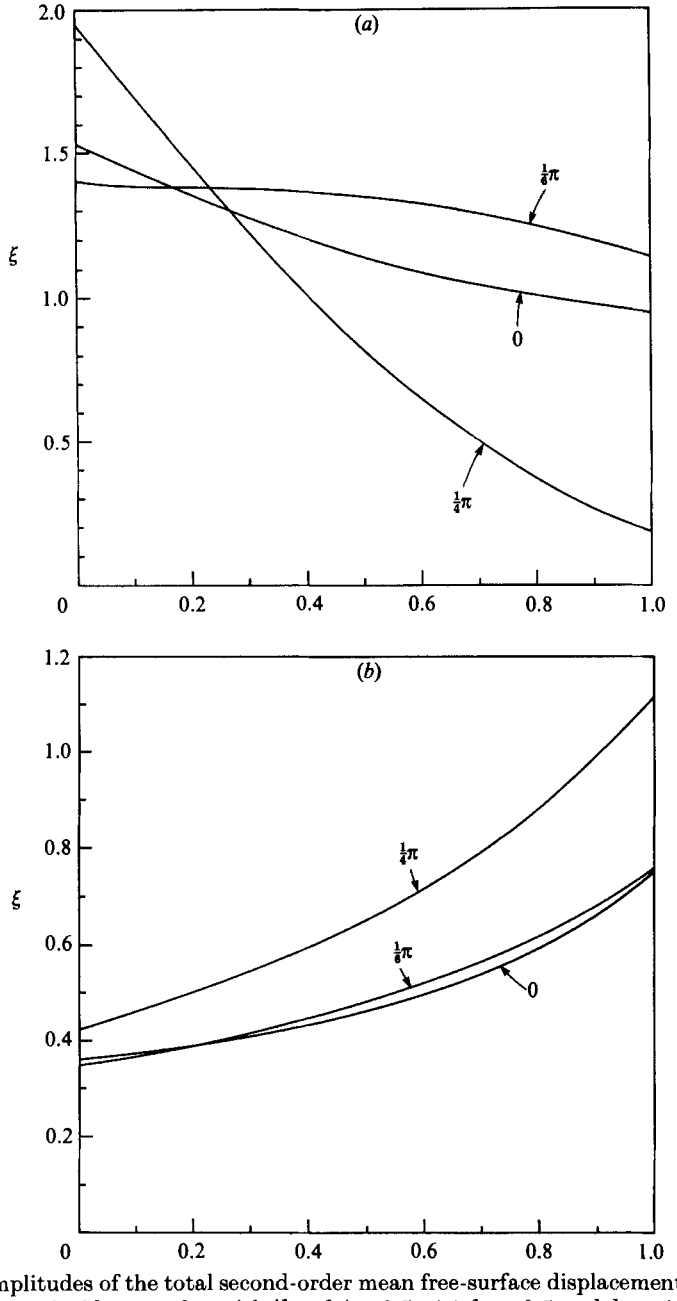

FIGURE 2. Amplitudes of the total second-order mean free-surface displacements, ξ, over the linear shelf for different incident angles with $|h_1 - h_0| = 0.5$: (*a*) $h_0 = 0.5$ and $h_1 = 1.0$; (*b*) $h_0 = 1.0$ and $h_1 = 0.5$.

for $X_0 < X < X_1$. The steady-state mean free-surface set-down in the constant-depth region remains a constant. Therefore,

$$\left.\frac{\mathrm{d}\xi_0}{\mathrm{d}X}\right|_{X_0-} = \left.\frac{\mathrm{d}\xi_0}{\mathrm{d}X}\right|_{X_1+} = 0$$

in the matching conditions (3.8) and (3.9).

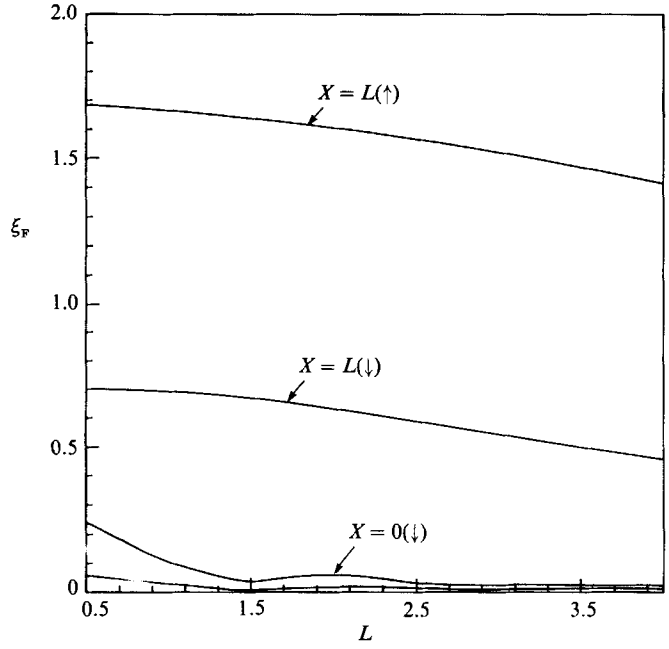

FIGURE 3. Amplitudes of free long waves at the edges of a linear shelf for normal incidence with $|h_1 - h_0| = 0.5$.

Numerical results are obtained by using the present solution method for $|h_1 - h_0| = 0.5$ and $L = (X_1 - X_0) = 1.0$ with $h_0 = 0.5$ and 1.0. The present numerical solutions were verified by the analytical solutions for the cases of normal incidence and increasing depth. With the finite-difference grid size $\Delta X = 0.02$, it is found that the present numerical results are the same as those calculated from the analytical solutions to within 0.1%. The amplitudes of ξ_F as defined by M & B are plotted in figure 1. Because different boundary conditions are used, the present results are quite different from those reported by M & B; particularly, slopes of $|\xi_F|$ are not zero at $X = X_0$ and X_1. The amplitudes of the total second-order mean free-surface displacements over the linear shelf are shown in figure 2. In figure 3, the free long-wave amplitudes at the edges of the shelf are plotted for normal incidence and different shelf width. The amplitudes of free long waves at the right edge, $X = X_1$, predicted by the present solution method are greater than those reported by M & B for the case of a negative shelf slope. If the shelf slope is positive, the reverse is true. Along the left edge of the shelf, $X = X_0$, the present solutions give smaller amplitudes of free long waves in both constant-depth regions than those given by M & B.

The research reported in this paper was supported, in part, by New York Sea Grant Institute through a research grant to Cornell University. The work was initiated while I was visiting the Delft Hydraulics Laboratory and the ISVA at the Technical University of Denmark. The financial support from both institutions is appreciated. I would like to thank Professor C. C. Mei for sending me Benmoussa's thesis. Discussions with M. W. Dingemans, J. K. Ksotense and I. Jonsson have been helpful.

REFERENCE

MEI, C. C. & BENMOUSSA, C. 1984 Long waves induced by short wave groups over an uneven bottom. *J. Fluid Mech.* **139**, 219–235.